Research Square

Preprints are preliminary reports that have not undergone peer review.
They should not be considered conclusive, used to inform clinical practice,
or referenced by the media as validated information.

Space Weather Radiation Assessment in Low Earth Orbit

Alessandro Bucci

alessandrobucci@hotmail.com

University of Rome Tor Vergata

Pio Ciro Aspetti

University of Rome Tor Vergata

Laura Mucciarelli

Andrea Malizia

University of Rome Tor Vergata

Research Article

Keywords: Low Earth Orbit, space radiation, radiation shielding, solar particle events, radiation monitoring, space weather forecasting, astronaut health, mission safety

Posted Date: February 27th, 2026

DOI: https://doi.org/10.21203/rs.3.rs-8900049/v1

License: This work is licensed under a Creative Commons Attribution 4.0 International License.
Read Full License

Additional Declarations: No competing interests reported.

Space Weather Radiation Assessment in Low Earth Orbit

Alessandro Bucci[1*], Pio Ciro Aspetti[1], Laura Mucciarelli and Andrea Malizia[1]

[1] *Department of Industrial Engineering, University of Rome Tor Vergata, Rome, (Italy)*

[*] Corresponding author: alessandrobucci@hotmail.com,

Abstract
As human activities in Low Earth Orbit (LEO) accelerate, a comprehensive understanding of radiation exposure risks driven by space weather phenomena is paramount for astronaut safety. This study examines the multifaceted radiation environment at orbital altitudes of approximately 400 km, focusing on how mission duration, shielding effectiveness, and solar volatility influence absorbed dose rates.

To complement high-fidelity computational simulations, this research introduces a simplified analytical scaling model. By deriving predictive dose formulas based on real-time data from 2024, a period defined by peak activity within Solar Cycle 25, this approach enables near-instantaneous risk assessment. This provides a computationally agile alternative to traditional, resource-intensive Monte Carlo methods without compromising the precision required for operational safety thresholds.

The findings underscore the vital role of advanced detection hardware and predictive space weather forecasting in facilitating proactive countermeasures, such as the strategic rescheduling of Extravehicular Activities (EVAs) and the utilization of hardened storm shelters during Solar Particle Events (SPEs). Beyond quantitative evaluation, this study advocates for an integrated radiation risk management framework. By synthesizing material innovation, adaptive mission design, and real-time predictive technologies, this framework enhances crew resilience in LEO and establishes a foundational blueprint for future deep-space exploration.

Keywords: Low Earth Orbit, space radiation, radiation shielding, solar particle events, radiation monitoring, space weather forecasting, astronaut health, mission safety.

1. Introduction

Low Earth Orbit (LEO), spanning altitudes from 160 to 2,000 km, represents a critical strategic domain for modern space activities, hosting the International Space Station (ISS) alongside expanding telecommunications and Earth-observation constellations. Although situated within the protective envelope of Earth's magnetosphere, this region remains highly susceptible to volatile space weather phenomena and a continuous background of Galactic Cosmic Rays (GCRs). This convergence of factors creates a dynamic and persistently challenging radiation environment for both biological and electronic systems.

While the magnetosphere significantly attenuates cosmic hazards, it does not entirely eliminate ionizing radiation risks for crews. At operational altitudes of approximately 400 km, the local environment is modulated by the complex interplay between geomagnetic shielding effectiveness and solar cycle periodicity. During Solar Cycle 25, the primary operational hazard is driven by Solar Particle Events (SPEs)—acute, unpredictable surges of high-flux protons and alpha particles. Although SPEs lack the heavy-ion diversity characteristic of GCRs, their extreme intensity can drive absorbed doses beyond established regulatory safety thresholds within narrow temporal windows, dramatically escalating oncogenic potential and neurological risks for crew members. Operational complexity is further heightened by the presence of the South Atlantic Anomaly (SAA). Due to the inherent offset and tilt of Earth's magnetic dipole, the inner Van Allen radiation belt penetrates deeply into LEO altitudes over the South Atlantic region. Consequently, spacecraft traversing this anomaly encounter a localized, intensified bombardment of trapped protons, making the SAA the dominant contributor to the cumulative radiation dose for platforms like the ISS.

This research provides a comprehensive assessment of radiation dose rates in LEO across a broad spectrum of space weather conditions, ranging from geomagnetically quiet intervals to extreme geomagnetic storms, classified according to the NOAA scales from minor (G1) to extreme (G5). Utilizing a simplified analytical scaling methodology—which integrates predictive modeling with empirical data—the study evaluates radiation exposure at a 400 km orbital altitude. These modeled values are subsequently compared against the equivalent dose rates experienced by astronauts to determine the efficacy of current safety protocols under heightened solar activity.

2. Materials and Methods

2.1 Radiation Exposure Assessment Methodology

Assessing radiation exposure in Low Earth Orbit (LEO) at approximately 400 km altitude requires analysing several key variables, including radiation intensity, conversion factors, geomagnetic shielding, and minimal residual atmospheric shielding. At this altitude, Earth's atmosphere provides negligible protection, making space radiation, including galactic cosmic rays (GCRs), solar particle events (SPEs), and trapped belt radiation, a primary concern.

MATLAB served as the primary computational platform for all data processing, numerical modeling, and visualization tasks throughout this study. A comprehensive suite of custom scripts and functions was developed to implement the complete radiation assessment workflow, encompassing space weather data ingestion, radiation transport calculations, shielding analysis, and time-resolved dosimetric evaluations. The assessment begins by converting incident radiation intensities into dose rates (measured in mSv/h) using established conversion coefficients based on particle type and energy. These dose rates are then adjusted for shielding effects from spacecraft materials, which serve as the main protective barrier in the absence of atmospheric shielding.

To estimate both instantaneous dose rates and cumulative exposure under varying space weather conditions, different simulations were performed. These simulations stochastically sample from known distributions of particle flux, shielding response, and exposure durations, enabling accurate modelling of radiation conditions during quiet periods and high-intensity solar events (Burrell at al., 1968). The analysis specifically targets the calculation of daily radiation dose rates (D) at 400 km for each simulated solar event, enabling comparison across space weather scenarios as follows:

$$D = I \cdot \alpha \cdot f(h) \cdot t \quad (1)$$

Variable	Description	Typical Unit	Note
I	Radiation Intensity	W/m²	Derived from NOAA GOES Satellite Data
α	Conversion Factor	m^2Sv/Wh	Standardizes radiation intensity into dose equivalents
f(h)	Dose Transmission Factor	sr	Depending on the specific altitude (h).
t	Total Time of Exposure	s	86,400 s for 24 hours

Table 1: Variables Description

By combining key variables, the daily radiation dose can be calculated offering valuable insight into the radiation risks associated as follows:

$$D_{day} = \sum_{j=1}^{M} D_j \quad (2)$$

with

- *j*: index of event.
- *M:* total number of radiation intensity events occurred during the day.

Once the daily dose is known, the cumulative total dose is determined by summing the daily doses over the entire mission duration. This cumulative dose represents the total radiation exposure as follows:

$$Cumulative\ Dose = \sum_{i=1}^{N} D_{day,i} \quad (3)$$

with

- i: index of the day.
- *N*: number of days representing the mission duration.
- $D_{day,i}$: daily dose for the i event.

2.2 Parameters

Dose rate of radiation from solar activity was determined by three primary parameters:

a) Solar radiation intensity (I)
b) Conversion factor (α)
c) Dose Transmission Factor (f(h)).

a) Solar Radiation Intensity (I)

Solar radiation intensity, denoted as *I* and measured in watts per square meter (W/m^2), quantifies the energy flux emitted by solar events and received at a specific location and it is expressed as:

$$I = \frac{P}{A} \quad (4)$$

with

- *P:* power emitted by the solar event (W)
- *A:* area over which the energy is distributed (m^2)

The solar radiation intensities utilized in the simulation were sourced from NOAA's Space Weather Prediction Center (SWPC) (https://www.ngdc.noaa.gov/stp/space-weather/swpc-products/daily_reports/solar_event_reports/), which facilitates the assessment of radiation hazards and the implementation of protective measures for aviation, astronaut safety, and critical infrastructure.

b) Conversion Factor (α)

Following the table above and formula (1) it is possible to define a strong relationship between Solar Radiation intensity (I) and Dose (D) through a conversion factor α measured in W/m^2h:

$$\alpha = \frac{D}{I \cdot f(h) \cdot t} = \frac{\dot{D}}{I \cdot f(h)} \quad (5)$$

where:

- *D*: radiation dose (Sv)
- *Ḋ*: radiation dose rate (Sv/h)
- *I*: solar radiation intensity (W/m^2)

The conversion factor α is not a fixed parameter, as its magnitude depends on a range of interrelated physical and environmental factors. These include the spectral composition of the incident radiation field, the type, charge, and energy distribution of the incoming particles, and the extent of atmospheric and geomagnetic shielding, which together determine how much of the primary cosmic or solar radiation reaches lower altitudes (Xu et al., 2021). Additionally, the biological effectiveness of different radiation components, such as protons, neutrons, and heavy ions, varies significantly, influencing how absorbed energy translates into effective dose. Because of these dependencies, the value of α differs according to altitude, geomagnetic latitude, and solar cycle phase, as well as the composition of the atmosphere and local geomagnetic field intensity (Larsen, 2023). In table 2 a representation of α values:

Altitude Regime	Conversion Factor (α)	Radiation Penetration	Description
Aviation Altitudes (9–12 km)	1	High X-ray penetration; low GCR and SEP contribution	At commercial flight altitudes, the atmosphere still provides substantial shielding, but enough thinning occurs for X-ray and secondary particle cascades to dominate. Galactic Cosmic Rays (GCR) and Solar Energetic Particles (SEP) are present but attenuated. This environment justifies using α ≈ 1 as a baseline reference.
Low Earth Orbit (LEO, ~400 km)	≈ 0.5	Reduced X-ray contribution;	In LEO, spacecraft are above nearly all atmospheric shielding but still partially protected by Earth's magnetosphere. X-ray attenuation is significant, while high-energy GCR and SEP become more relevant. The

Altitude Regime	Conversion Factor (α)	Radiation Penetration	Description
		increased GCR and SEP flux	mixed-field environment leads to a lower α, reflecting the reduced biological effectiveness per unit solar energy input.
Lunar Orbit (~400,000 km)	≈ 0.01	Negligible X-ray shielding; dominant GCR and SEP exposure	At lunar distances, there is no atmospheric shielding and only minimal geomagnetic protection. X-ray contributions become negligible compared to the overwhelming presence of GCR and SEP. The conversion factor drops sharply because the solar irradiance–to–dose relationship is no longer dominated by photon interactions but by high-energy particle fluxes with different biological weighting.

Table 2: Conversion Factor α

Specifically, the value α = 0.4 m^2Sv/Wh was adopted as an approximate reference value rather than a fixed physical constant. It serves to simplify the relationship between radiation intensity and the resulting equivalent dose within the modelling framework. This assumption provides a practical baseline for estimating dose under varying space weather and atmospheric conditions, without requiring detailed knowledge of the radiation spectrum or particle transport mechanism ensuring flexibility in adapting theoretical frameworks to complex, real-world scenarios.

c) Dose Transmission Factor

Earth's atmosphere serves as a natural barrier against ionizing radiation, significantly reducing the absorbed dose at ground level. The dose transmission factor T(h) is a dimensionless parameter that quantifies the fraction of deep-space radiation dose that reaches a given altitude h, influenced by both natural and artificial barriers. It represents the fraction of incoming deep-space radiation transmitted to a given altitude h through the Earth's atmospheric layers, spacecraft shielding, or both, for ionizing radiation sources such as cosmic rays and solar radiation. Mathematically, it can be formulated as follows:

$$f(h) = \frac{D_{actual}}{D_{deepspace}} (6)$$

Where

- D_{actual}: radiation dose experienced after shielding.
- $D_{deepspace}$: radiation dose without any shielding.
- $f(h)$: dose transmission factor at altitude h.

In Table 3, the dose transmission factor values at different altitudes:

Altitude	Shielding Factor f(h)	Radiation Penetration	Description
Ground Level	~ 0.01	1% of incoming radiation reaches the surface	The atmosphere effectively blocks most cosmic and solar radiation.
Aviation Altitudes (9–12 km)	0.1 – 0.2	10–20% of solar radiation penetrates	Radiation exposure increases as atmospheric shielding decreases.
Lower Thermosphere (~100 km)	0.5 – 1.0	Nearly all incoming radiation reaches this altitude	The atmosphere becomes very thin, providing minimal shielding against radiation.
Low Earth Orbit (~400 km)	~ 2.0	Twice the deep-space radiation dose compared to Earth	Trapped particle radiation in the Van Allen belts results in a dose exceeding the deep-space reference level.

Table 3: Dose Transmission Factor f(h)

The effectiveness of atmospheric shielding against space radiation is strongly influenced by altitude, geographic location, and the level of geomagnetic activity. At an altitude of approximately 400 km, typical of Low Earth Orbit (LEO), the Earth's atmosphere

provides negligible protection. At this altitude, the geomagnetic field plays a dual role: it deflects a portion of incoming galactic and solar particles, but simultaneously traps others in the Van Allen belts, resulting in a net dose that exceeds the deep-space reference level at LEO.

During periods of normal space weather, the dose transmission factor T(h) at 400 km is typically around 2.0, reflecting the absence of significant atmospheric shielding and the net enhancement of radiation from trapped particles in the Van Allen belts. However, during geomagnetic storms, the Earth's magnetic field weakens, enabling a greater flux of high-energy particles, including galactic cosmic rays and solar energetic particles, to penetrate near-Earth space. As a result, the dose transmission factor increases, along with the associated radiation dose.

Moderate solar storms, often triggered by M-class solar flares and moderate coronal mass ejections (CMEs), lead to a notable increase in the influx of high-energy protons. Under such conditions, the dose transmission factor can rise to values between 3.0 and 4.0. This corresponds to an estimated radiation dose of approximately 3 to 5 millisieverts per day. In the case of stronger geomagnetic storms, typically associated with X-class solar flares and fast, high-energy CMEs, the dose transmission factor may increase further, reaching values between 5.0 and 6.0. Such conditions can produce daily radiation doses in the range of 6 to 10 millisieverts.

In rare but extreme events, such as those comparable to the 1859 Carrington Event, the dose transmission factor can exceed 10. These powerful solar particle events are characterised by exceptionally high proton fluxes and can result in daily radiation doses estimated between 50 and 100 millisieverts. Table 4 below summarises these values across geomagnetic storm categories:

Altitude	No Solar Storm	G1 (Minor)	G2 (Moderate)	G3 (Strong)	G4 (Severe)	G5 (Extreme)
f(h) @ 400 km	2.0	~2.2	~2.5	~3.0	~4.0	≥5.0

Table 4: Dose Transmission Factor f(h) Vs Geomagnetic Storm Amplitude

These variations in the dose transmission factor clearly illustrate how geomagnetic storms significantly exacerbate radiation risks, particularly at higher altitudes where atmospheric protection is minimal. For both aviation and space operations, the ability to accurately model these fluctuations is essential

3. Results

3.1 Scenarios Comparison

The study analysed six unique scenarios for the year 2024, consisting of a reference scenario and five additional scenarios that varied in geomagnetic storm intensity as shown in Figure 1,2 and 3. These intensities were classified according to the NOAA G-scale, ranging from G1 (minor) to G5 (extreme), and were accompanied by an increasing number of active regions (AR). This classification provided insight into the potential radiation effects associated with different levels of geomagnetic disturbances.

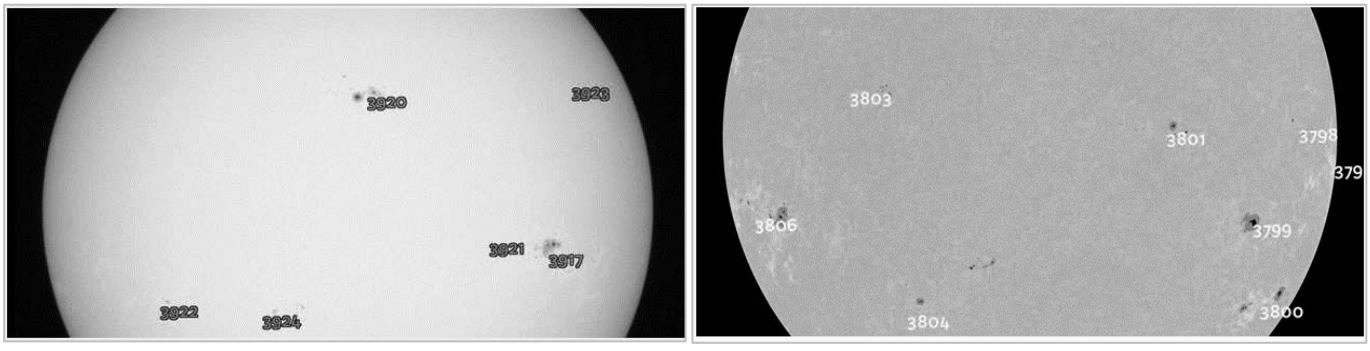


Figure 1: Reference Scenario - Dec 13th, 2024 and Scenario 1 - Aug 31st, 2024 **(G1 Class)**

(Space Weather Live 2024/12/13 and 2024/08/31)

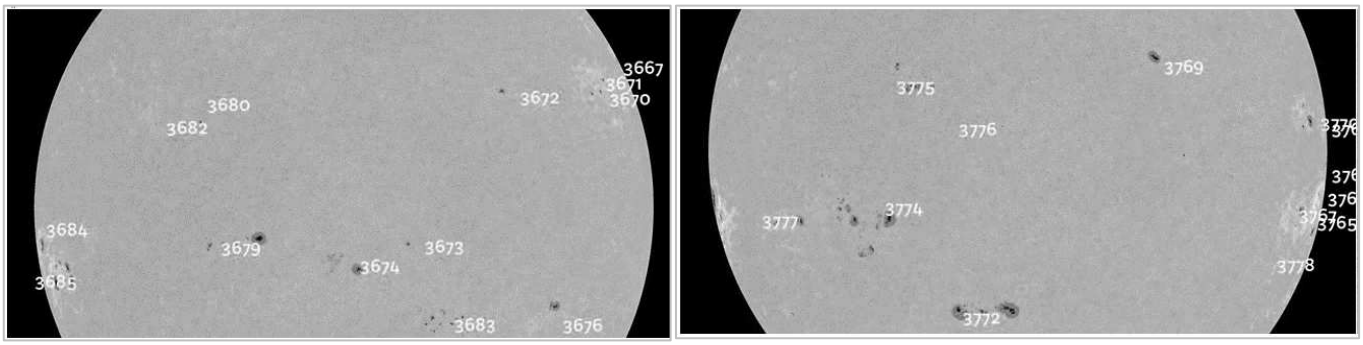


Figure 2: Scenario 2 - May 17th, 2024 **(G2 Class)** and Scenario 3 - Aug 4th, 2024 **(G3 Class)**
(Space Weather Live 2024/5/17 and 2024/08/04)

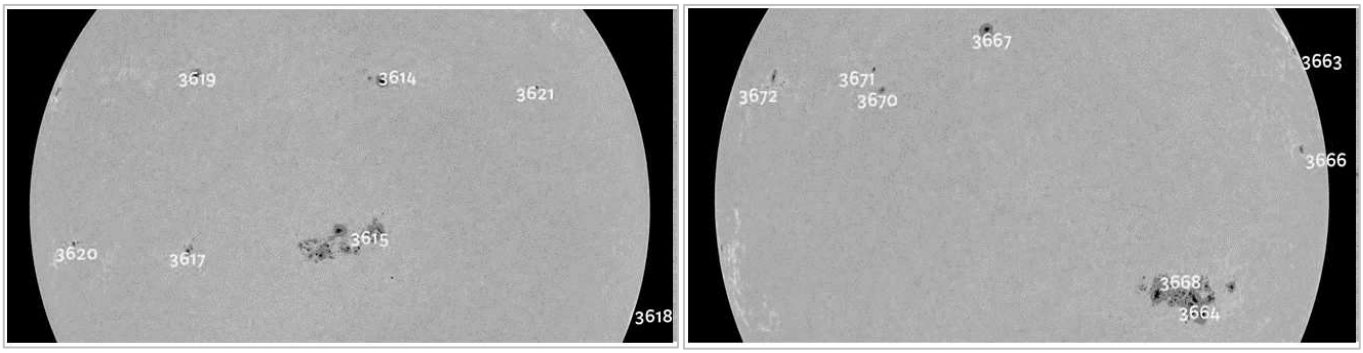
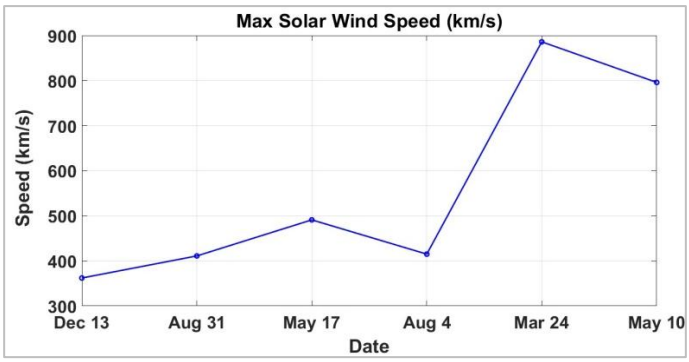


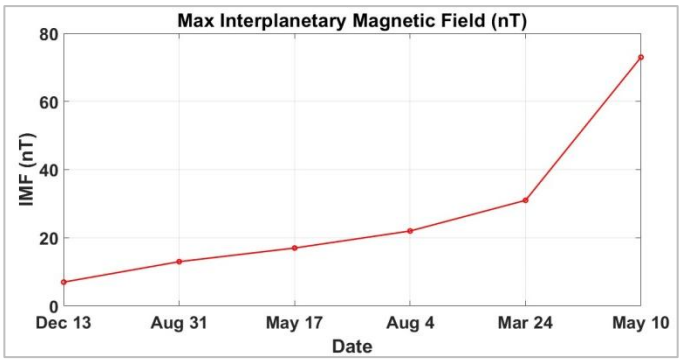
Figure 3: Scenario 4 - Mar 24th, 2024 **(G4 Class)** and Scenario 5 - May 10th, 2024 **(G5 Class)**
(Space Weather Live 2024/03/24 and 2024/05/10)

The scenarios identified critical parameters, including solar wind speed, interplanetary magnetic field strength, and southward Bz components, all of which had a direct impact on radiation dose at an altitude of 400 km in low Earth orbit (LEO) as listed in Table 5 and Figure 4.

Scenario	Day	G Class	Max Solar Wind Speed (km/s)	Max IMF (nT)	Southward Bz (nT)	Dst Index (nT)	Kp Index
Reference Scenario	Dec 13th, 2024	-	362	7		-13	~2
Scenario 1	Aug 31st, 2024	G1	411	13	-12	-12	~5
Scenario 2	May 17th, 2024	G2	491	17	-15	-99	~6
Scenario 3	Aug 4th, 2024	G3	415	22	-17	-101	~7
Scenario 4	Mar 24th, 2024	G4	886	31	-24	-128	~8+
Scenario 5	May 10th, 2024	G5	796	73	-50	-351	~9-

Table 5: Scenarios Data





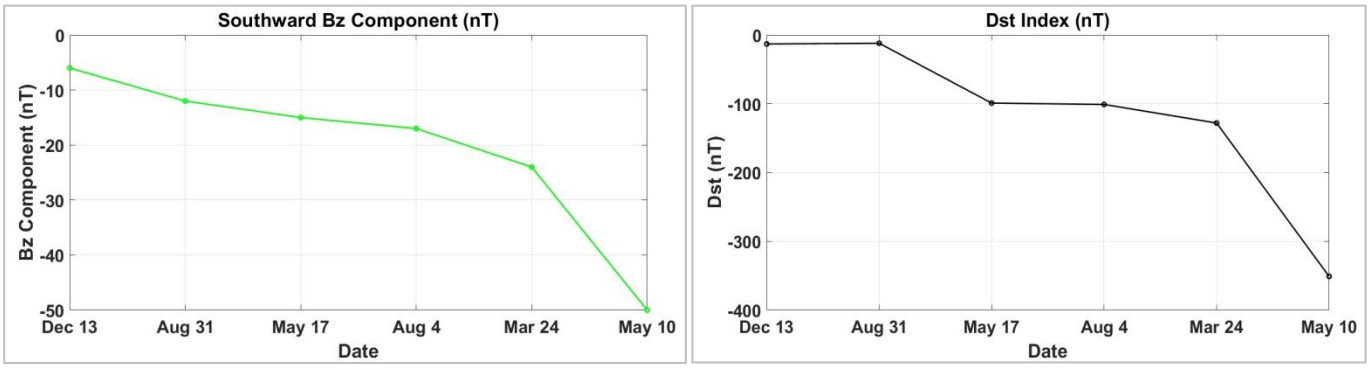


Figure 4: Scenarios Data

The starting point of the study was calculating the daily radiation doses for the different scenarios as indicated in Table 6 and Figure 5:

Scenario	Day	G Class	Daily Dose @ 400 km (mSv/d)
Reference Scenario	Dec 13th, 2024	-	0.969
Scenario 1	Aug 31st, 2024	G1	1.901
Scenario 2	May 17th, 2024	G2	2.885
Scenario 3	Aug 4th, 2024	G3	3.263
Scenario 4	Mar 24th, 2024	G4	6.121
Scenario 5	May 10th, 2024	G5	29.640

Table 6: Cumulative Daily Dose Comparison

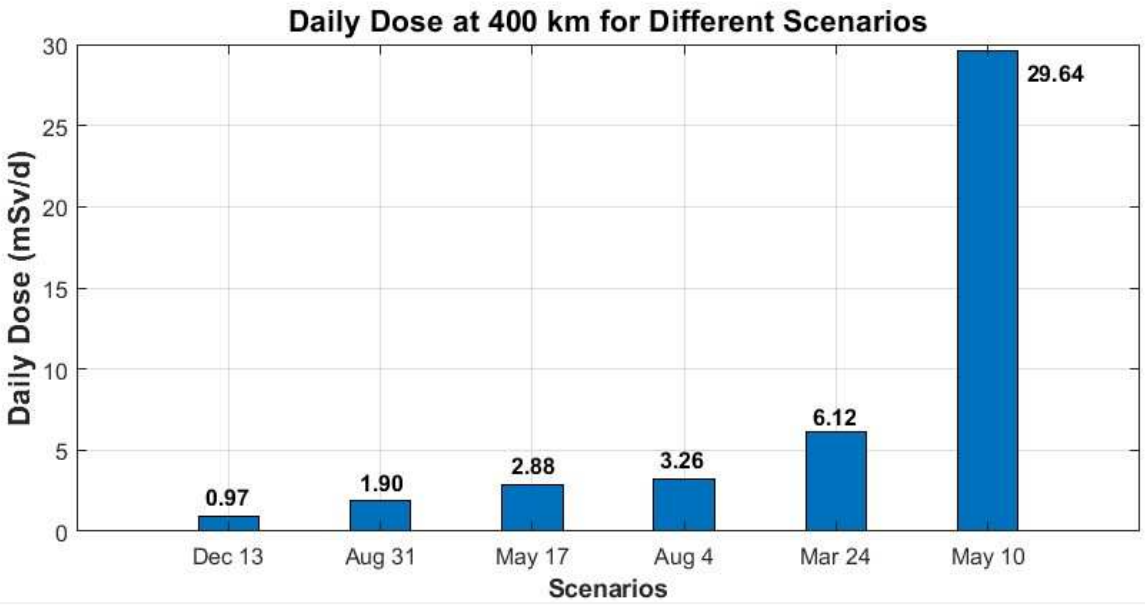


Figure 5: Daily Dose Comparison at 400 km for the Analysed Scenarios

3.2 Time Allocation for Astronauts

Astronauts aboard the International Space Station (ISS) adhere to a regimented daily schedule that integrates scientific tasks, spacecraft maintenance, physical exercise, and personal care, all distributed across functionally distinct modules. Most work hours (typically 8 to 10 hours per weekday) are spent within laboratory modules such as Destiny (NASA), Columbus (ESA), and Kibo (JAXA), where multidisciplinary research is conducted. These modules (see Figure 6), while essential for mission productivity, provide limited radiation protection, with an estimated dose attenuation of approximately 15–20% due to their thin structural walls and relatively low internal mass (Berger, 2008).

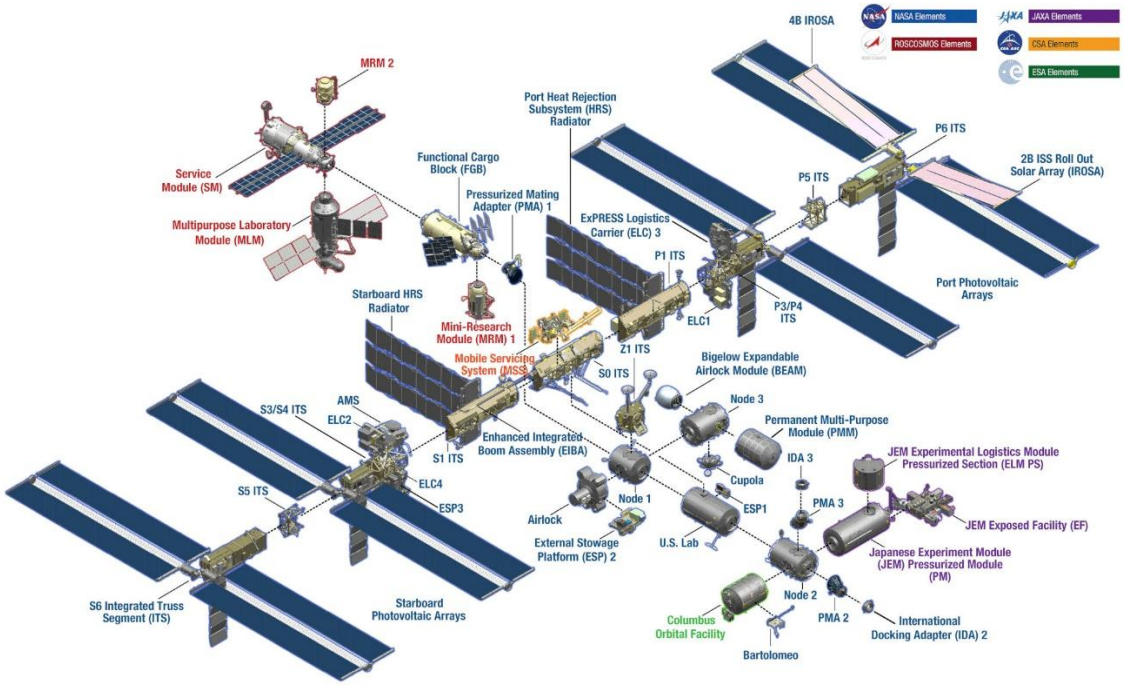


Figure 6: International Space Station (NASA 2025)

Extravehicular activities (EVAs), though infrequent, constitute one of the most radiation-intensive operational components. Each EVA typically lasts between 6 and 7.5 hours and is conducted outside the protective shielding of the ISS. Over a standard six-month mission, astronauts may accumulate between 20 and 40 hours of EVA time (Barratt & Pool, 2008; NASA, 2020). Pre-EVA preparations are carried out in specialized airlock modules such as Quest (United States) or Pirs (Russia), where procedures including pre-breathing and equipment checks are performed. These airlocks offer minimal shielding from space radiation, with only a modest reduction in dose (approximately 15%) compared to interior pressurized environments (Sato et al., 2011).

To mitigate the deleterious physiological effects of prolonged exposure to microgravity, astronauts engage in approximately 2.5 hours of physical exercise per day. This activity takes place primarily in the Tranquility module (Node 3), which houses the T2 treadmill and the Advanced Resistive Exercise Device (ARED). The module provides moderate radiation protection, aided by the presence of stored hardware and systems infrastructure, which together afford a dose reduction of roughly 25% (Loehr et al., 2015).

Rest and sleep are typically undertaken in private crew quarters located in Harmony (Node 2) and Zvezda (Russian segment). While Harmony offers basic accommodations, Zvezda provides enhanced radiation shielding, achieving dose reductions of up to 40–50%. This increased protection is attributed to both thicker module walls and the strategic placement of consumables (such as food and water) which act as passive shielding barriers (Sato et al., 2011). Additional daily activities, including hygiene, meals, and personal communication, are conducted in shared modules such as Unity and Zvezda. These functions, although operationally secondary, are vital for maintaining psychological health and morale during extended missions (Barger et al., 2014). The overall distribution of astronaut time across ISS modules reflects a deliberate balance between mission-critical tasks, physiological

maintenance, and radiation risk mitigation, offering valuable insights into the design and planning of future long-duration spaceflights beyond low Earth orbit and, considering mean values, are represented in Table 7.

Activity	Module(s)	Time Allocation (hrs/day)	Shielding Factor (% Dose Reduction)
Extravehicular Activities (EVAs)	Outside ISS	0,50	0%
Work and Research Activities (WRAs)	Destiny, Columbus, Kibo	8,50	15%
Exercise Activities (EAs)	Tranquility	3,00	25%
Sleep and Rest Activities (SRAs)	Harmony and Zvezda	8,00	40%
Meals & Personal Time Activities (MPTAs)	Unity, Zvezda	2,50	40%
EVA Preparation Activities (EPAs)	Quest Airlock, Pirs	0,50	15%
Transit and General Movement Activities (TGMAs)	All pressurized modules	1,00	25%

Table 7: Mean Time Allocation for Different Pressurized Modules

3.3 Variability of Shielding During Geomagnetic Storm Events

Radiation dose rates within the International Space Station (ISS) are influenced not only by structural and passive shielding but also by the space weather environment, particularly geomagnetic storm activity and associated solar particle events (SPEs). The Zvezda service module, designed for long-duration human habitation, benefits from both its structural thickness and the strategic placement of hydrogen-rich consumables, providing effective passive shielding. During periods of relatively low solar activity (i.e., no geomagnetic storm), the dominant radiation exposure arises from galactic cosmic rays (GCRs), resulting in typical absorbed dose rates of 1.3–1.5 mSv/day in unshielded areas of the ISS (Cucinotta et al., 2006; Sato et al., 2011). In contrast, Zvezda's crew quarters, with enhanced shielding, exhibit dose rates closer to 0.8–1.0 mSv/day, reflecting a 30–50% reduction in dose equivalent under nominal conditions (Berger, 2008).

During solar storm events, categorized by NOAA's Space Weather Scale from G1 (minor) to G5 (extreme), the nature and effectiveness of shielding change due to the influx of high-energy protons and heavier ions emitted by solar flares and coronal mass ejections (CMEs). These solar particles differ significantly from GCRs in energy and penetration, with lower-energy protons (<100 MeV) being more effectively attenuated by spacecraft shielding. Consequently, Zvezda's shielding factor (defined as the percentage reduction in dose compared to unshielded environments) actually increases in relative effectiveness during low-to-moderate storm activity, especially for SPE-dominated radiation fields (Simonsen et al., 2020) as indicated in Table 8, here below.

G Class	Typical External Dose (mSv/day)	Zvezda Dose (mSv/day)	% Shielding Factor	% Mean Shielding Factor	% Change
No Storm	1.3–1.5	0.8–1.0	33–46%	39.5%	-
G1 (Minor)	1.7–2.0	1.0–1.2	41–50%	45.5%	+15.2%
G2 (Moderate)	2.5–3.0	1.3–1.5	40–50%	45%	-1.1%
G3 (Strong)	3.5–5.0	2.0–2.5	43–50%	46.5%	+3.3%
G4 (Severe)	6.0–8.0	3.5–4.5	44–53%	48.5%	+4.3%
G5 (Extreme)	9.0–12.0+	6.0–7.0	38–50%	44%	-9.2%

Table 8: % Mean Shielding Factor

For the simulations it will be used a mean value and it will be assumed the all the pressurized modules have a structural behaviour same as the Zvezda module changing their behaviour as described in the last column of the table above.
In general, the data in the table reflect that the absolute dose levels rise sharply during stronger solar storms, but the relative shielding factor often remains within a 38–53% reduction range, depending on shielding material configuration and the energy spectrum of the incident particles.

The slight drop in shielding performance beyond G4–G5 is due to high-energy solar protons (>150 MeV), which have greater penetration capability and are less attenuated by standard aluminium and polyethylene shielding (Simonsen et al., 1990). Furthermore, during intense solar particle events, shielding design becomes critical not only for dose reduction but also for peak dose rate mitigation, especially in scenarios where astronauts must shelter in place for hours. Zvezda's use of stowage-based shielding (placing water bags and food rations around sleeping quarters) has proven especially valuable during SPEs with steep energy cutoffs, where even simple hydrogenous materials can block the majority of particle flux under 100 MeV (Simonsen et al., 2020).

3.4 Daily Dose Comparison in LEO for Different Activities and ISS Modules

Extravehicular Activities (EVAs)
Extravehicular activities (EVAs) conducted outside the International Space Station (ISS), typically via the Quest Airlock, involve astronauts spending an average of 0.50 hours per day in a highly exposed environment. These operations are critical for maintenance, installation, and repair tasks that cannot be performed from within the spacecraft. However, EVAs present significant radiological risks due to the absence of any substantial shielding, resulting in a 0% dose reduction from galactic cosmic rays (GCRs) and solar particle events (SPEs). The lack of effective shielding during these activities renders astronauts directly exposed to the ambient space radiation environment, contributing disproportionately to their cumulative mission dose. Consequently, minimizing EVA duration and scheduling such activities during periods of low solar activity are essential strategies in radiation risk management for long-duration missions.
In Table 9 the equivalent dose @400 km for EVA:

Scenario	G Class	Deep-space Daily Dose @ 400 km (mSv)	Mean Shielding Factor (%)	EVA Daily Dose @ 400 km (mSv)	Allocated Time (hour)	EVA Equivalent Dose @ 400 km (mSv)
Reference	-	0.969	0%	0.969	0.5	**0.0202**
Scenario 1	G1	1.901	0%	1.901	0.5	**0.0396**
Scenario 2	G2	2.885	0%	2.885	0.5	**0.0601**
Scenario 3	G3	3.263	0%	3.263	0.5	**0.0680**
Scenario 4	G4	6.121	0%	6.121	0.5	**0.1275**
Scenario 5	G5	29.640	0%	29.640	0.5	**0.6175**

Table 9: Equivalent Dose @400 km for EVA

Work and Research Activities (WRAs)
Astronauts typically spend an average of 8.50 hours per day conducting scientific experiments and technical operations within the pressurized laboratory modules aboard the ISS, including Destiny (NASA), Columbus (ESA), and Kibo (JAXA). These modules are equipped with standard spacecraft shielding, which provides a mean radiation dose reduction of approximately 15%. Although this shielding offers some protection against space radiation, particularly against lower-energy components of galactic cosmic rays (GCRs) and secondary radiation, it is only partially effective. As such, extended daily exposure within these environments still contributes significantly to the crew's total radiation burden over the course of a mission.
In Table 10 the equivalent dose @400 km for WRAs:

Scenario	G Class	Deep-space Daily Dose @ 400 km (mSv)	Mean Shielding Factor (%)	WRAs Daily Dose @ 400 km (mSv)	Allocated Time (hour)	WRAs Equivalent Dose @ 400 km (mSv)
Reference	-	0.969	15%	0.824	8.5	**0.292**
Scenario 1	G1	1.901	17.28%	1.573	8.5	**0.557**
Scenario 2	G2	2.885	17.09%	2.392	8.5	**0.848**
Scenario 3	G3	3.263	17.66%	2.686	8.5	**0.951**
Scenario 4	G4	6.121	18.42%	4.995	8.5	**1.770**
Scenario 5	G5	29.640	16.71%	24.694	8.5	**8.740**

Table 10: Equivalent Dose @400 km for Work and Research Activities

Exercise Activities (EAs)
Crewmembers aboard the International Space Station allocate approximately 3.00 hours per day to physical exercise within the Tranquility module (Node 3). This activity is essential for preserving bone density and muscle mass during long-duration spaceflight, using specialized equipment such as the T2 treadmill, Advanced Resistive Exercise Device (ARED), and Cycle Ergometer with Vibration Isolation and Stabilization (CEVIS).

Tranquility offers moderate structural shielding, contributing to a mean dose reduction of about 25%. While this shielding provides partial mitigation against ambient space radiation, the relatively long duration of daily exercise means that cumulative exposure from this location remains a notable component of the overall mission dose. Optimizing exercise scheduling and potentially enhancing localized shielding around high-use areas may help further reduce radiation risk during these necessary physical activities. In Table 11 the equivalent dose @400 km for exercise activities in the Tranquillity module:

Scenario	G Class	Deep-space Daily Dose @ 400 km (mSv)	Mean Shielding Factor (%)	EAs Daily Dose @ 400 km (mSv)	Allocated Time (hour)	EAs Equivalent Dose @ 400 km (mSv)
Reference	-	0.969	25%	0.727	3	**0.091**
Scenario 1	G1	1.901	28.80%	1.355	3	**0.169**
Scenario 2	G2	2.885	28.48%	2.062	3	**0.258**
Scenario 3	G3	3.263	29.43%	2.303	3	**0.288**
Scenario 4	G4	6.121	30.68%	4.244	3	**0.531**
Scenario 5	G5	29.640	27.86%	21.392	3	**2.674**

Table 11: Equivalent Dose @400 km for Exercise Activities

Sleep and Rest Activities (RSAs)

Astronauts aboard the ISS typically allocate 8.00 hours per day for sleep and rest, primarily within private crew quarters located in the Harmony and Zvezda modules. These compartments are situated in areas with relatively enhanced structural shielding, offering a mean radiation dose reduction of approximately 40%. As one of the longest continuous activities during a 24-hour cycle, sleep provides a critical opportunity for both physiological recovery and radiation exposure mitigation. The protective environment of these modules contributes significantly to reducing the crew's cumulative radiation dose. Optimizing sleep locations based on radiation shielding effectiveness—especially during heightened solar activity—remains an important consideration in ISS habitat design and crew scheduling.

In Table 12 the effective dose rate @400 km for RSAs:

Scenario	G Class	Deep-space Daily Dose @ 400 km (mSv)	Mean Shielding Factor (%)	RSAs Daily Dose @ 400 km (mSv)	Allocated Time (hour)	RSAs Equivalent Dose @ 400 km (mSv)
Reference	-	0.969	39.5%	0.587	8	**0.196**
Scenario 1	G1	1.901	45.5%	1.036	8	**0.345**
Scenario 2	G2	2.885	45%	1.587	8	**0.529**
Scenario 3	G3	3.263	46.5%	1.744	8	**0.581**
Scenario 4	G4	6.121	48.5%	3.153	8	**1.051**
Scenario 5	G5	29.640	44%	16.598	8	**5.533**

Table 12: Equivalent Dose @400 km for Rest and Sleep Activities

Meals and Personal Time Activities (MPTAs)

Astronauts typically spend around 2.50 hours per day on meals, personal hygiene, communication, and leisure activities within the Unity (Node 1) and Zvezda modules. These areas serve as key living quarters and are designed for both functionality and crew well-being. The structural configuration and material composition of these modules provide a relatively higher level of shielding, resulting in a mean radiation dose reduction of approximately 40%**.** This enhanced protection makes them comparatively safer zones within the ISS, contributing to overall dose management by offering periods of reduced exposure. Strategic use of these more shielded areas during solar particle events (SPEs) or when not engaged in critical mission operations may further mitigate radiation risks for the crew. In Table 13 the effective dose @400 km for MPTAs:

Scenario	G Class	Deep-space Daily Dose @ 400 km (mSv)	Mean Shielding Factor (%)	MPTAs Daily Dose @ 400 km (mSv)	Allocated Time (hour)	MPTAs Equivalent Dose @ 400 km (mSv)
Reference	-	0.969	39.5%	0.587	2.5	**0.061**
Scenario 1	G1	1.901	45.5%	1.036	2.5	**0.108**
Scenario 2	G2	2.885	45%	1.587	2.5	**0.165**
Scenario 3	G3	3.263	46.5%	1.744	2.5	**0.182**
Scenario 4	G4	6.121	48.5%	3.153	2.5	**0.328**
Scenario 5	G5	29.640	44%	16.598	2.5	**1.729**

Table 13: Equivalent Dose @400 km for Rest and Sleep Activities

Eva Preparation Activities (EPAs)

Astronauts typically spend about 0.50 hours per day on preparation for extravehicular activities (EVAs) within the Quest (U.S.) and Pirs (Russian) airlocks. These procedures include space suit checks, pre-breathing protocols, and decompression steps necessary for safe transition to the vacuum of space. The airlocks provide limited shielding, with a mean radiation dose reduction of approximately 15%. While the duration of this activity is relatively short, the proximity to external structures and lower shielding effectiveness mean it contributes modestly but non-negligibly to the total radiation exposure. Managing exposure during this transitional phase is essential, particularly during periods of elevated radiation risk, such as solar particle event.

In Table 14 the effective dose @400 km for EPAs:

Scenario	G Class	Deep-space Daily Dose @ 400 km (mSv)	Mean Shielding Factor (%)	EPAs Daily Dose @ 400 km (mSv)	Allocated Time (hour)	EPAs Equivalent Dose @ 400 km (mSv)
Reference	-	0.969	15%	0.824	0.5	**0.017**
Scenario 1	G1	1.901	17.28%	1.573	0.5	**0.033**
Scenario 2	G2	2.885	17.09%	2.392	0.5	**0.050**
Scenario 3	G3	3.263	17.66%	2.686	0.5	**0.056**
Scenario 4	G4	6.121	18.42%	4.995	0.5	**0.104**
Scenario 5	G5	29.640	16.71%	24.694	0.5	**0.514**

Table 14: Equivalent Dose @400 km for Eva Preparation Activities

Transit and General Movement Activities (TGMAs)

Astronauts spend approximately 1.00 hour per day in transit between modules and performing general coordination tasks across all pressurized segments of the ISS. This activity includes movement through connecting nodes, equipment transfers, and brief interactions across workspaces. Due to the mixed shielding characteristics of the various modules, this activity is associated with a mean radiation dose reduction of approximately 25%. Although brief compared to other daily activities, general movement exposes crew members to a representative cross-section of the station's radiation environment. Accurate modelling of this exposure helps refine total mission dose estimates and supports informed decisions in station layout planning and crew scheduling.

For the transit and general movement phase lasting around 1 hour a day through the different pressurized modules of the ISS, we have the values indicated in Table 15:

Scenario	G Class	Deep-space Daily Dose @ 400 km (mSv)	Mean Shielding Factor (%)	TGMAs Daily Dose @ 400 km (mSv)	Allocated Time (hour)	TGMAs Equivalent Dose @ 400 km (mSv)
Reference	-	0.969	25%	0.727	1	**0.030**
Scenario 1	G1	1.901	28.80%	1.355	1	**0.056**
Scenario 2	G2	2.885	28.48%	2.062	1	**0.086**
Scenario 3	G3	3.263	29.43%	2.303	1	**0.096**
Scenario 4	G4	6.121	30.68%	3.153	1	**0.131**

Scenario 5	G5	29.640	27.86%	21.392	1	**0.891**

Table 15: Equivalent Dose @400 km for Transit and General Movement Activities

Following the data obtained in the tables presented in the previous paragraph, and considering the % time allocated for the different activities as shown in Figure 7,

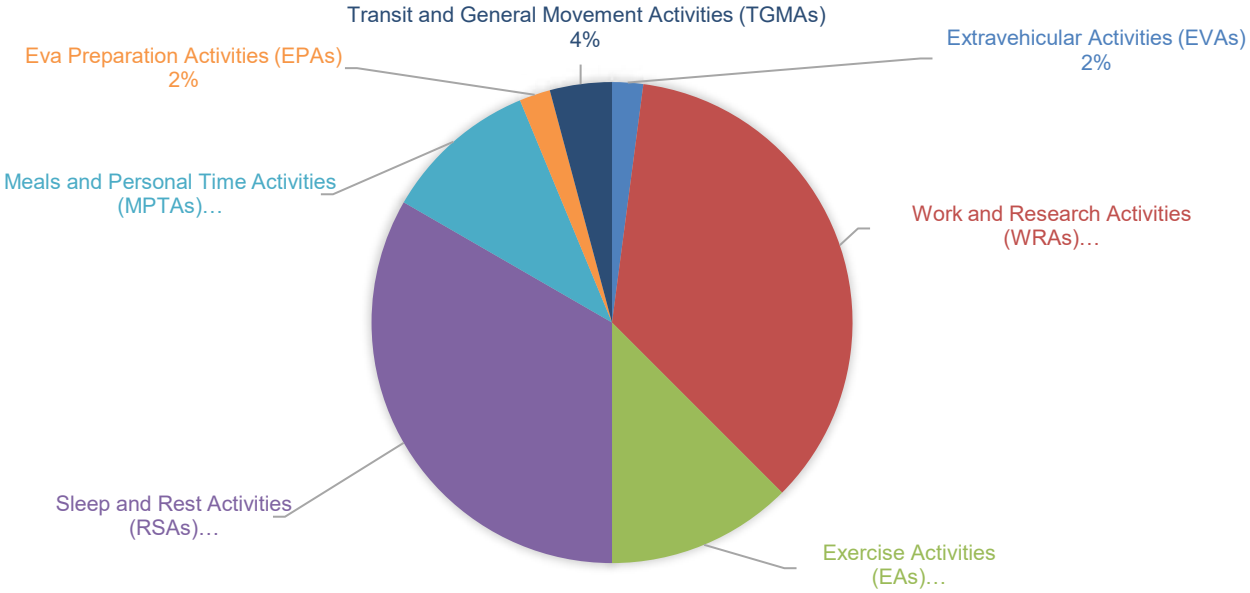


Figure 7: Time Allocation for Astronauts

it is possible to estimate the daily effective dose assumed by the crew in 24 hours/day for the different scenarios at 400 km as listed in Table 16:

Scenario	G Class	Equivalent Dose (mSv)							
		EVA	WRAs	EAs	RSAs	MPTAs	EPAs	TGMAs	TOTAL
Reference	-	0.0202	0.292	0.091	0.196	0.061	0.017	0.030	**0.7072**
Scenario 1	G1	0.0396	0.557	0.169	0.345	0.108	0.033	0.056	**1.3076**
Scenario 2	G2	0.0601	0.848	0.258	0.529	0.165	0.050	0.086	**1.9961**
Scenario 3	G3	0.0680	0.951	0.288	0.581	0.182	0.056	0.096	**2.2220**
Scenario 4	G4	0.1275	1.770	0.531	1.051	0.328	0.104	0.131	**4.0425**
Scenario 5	G5	0.6175	8.740	2.674	5.533	1.729	0.514	0.891	**20.698**

Table 16: Equivalent Total Daily Dose @400 km for Different Modules and Activities

The reference scenario (December 13, 2024), representing quiet space-weather conditions, yields a total equivalent dose of 0.707 mSv. This value is consistent with typical daily exposures in low Earth orbit during periods of minimal geomagnetic disturbance and serves as the baseline for comparison.

Under Scenario 1 (August 31, 2024), associated with a G1 geomagnetic storm, the total equivalent dose increases to 1.308 mSv, nearly doubling the reference level. This demonstrates that even relatively weak geomagnetic activity can significantly elevate radiation exposure, particularly during orbital passes through regions such as the South Atlantic Anomaly or higher-latitude segments of the orbit. As storm intensity increases, the radiation environment becomes progressively harsher. Scenario 2 (May 17, 2024), corresponding to a G2 storm, results in a total dose of 1.996 mSv, while Scenario 3 (August 4, 2024), a G3 event, produces 2.222 mSv. Both scenarios yield exposures roughly three times higher than the baseline, highlighting a clear upward trend with increasing geomagnetic disturbance. A more substantial escalation occurs in Scenario 4 (March 24, 2024), linked to a

G4 storm, where the total equivalent dose reaches 4.043 mSv. At this level, operational constraints become more pronounced, as exposures approach or exceed typical daily or short-term limits depending on mission-specific radiation protection standards. During such events, it is generally advisable to curtail extravehicular activities and relocate crew to more shielded ISS modules.

The most extreme case, Scenario 5 (May 10, 2024), associated with a G5 geomagnetic storm, results in a total equivalent dose of 20.698 mSv. This value is nearly 30 times higher than the reference scenario and may exceed established short-term exposure limits, particularly for EVA operations or time spent in lightly shielded areas. Under such conditions, mission protocols would require immediate implementation of storm-sheltering procedures and postponement of non-critical activities.

4. Analysis

4.1 Analysis of Events

The objective of this event analysis was to estimate the annual dose for the year 2024 that an astronaut on a Low Earth Orbit (LEO) mission, could theoretically receive if working every day of the year at 400 km of altitude. Specifically, year 2024 was analysed in detail and for each day was reported in the Table 17, the Kp value:

Kp Matrix	1	2	3	4	5	6	7	8	9	10	11	12	13	14	15	16	17	18	19	20	21	22	23	24	25	26	27	28	29	30	31
Jan 24	4	3-	3+	3-	2	1	0+	2	2+	2+	2	1+	1-	2	2+	3-	1+	2+	3-	2+	2	3+	3-	3+	2+	2	2+	3	3-	2+	2+
Feb 24	2	1	1-	3	3-	3	1+	2-	3	2+	4+	2+	4-	3	1+	2	2	3+	0+	2+	1+	2-	1+	2+	3	3	4+	2	2-		
Mar 24	3-	2+	6+	4	3-	3	4-	4-	4	2+	2	2+	3+	3	3+	1-	0+	3-	3-	2+	5-	3+	6-	8+	5	3	3	3-	2-	2-	4-
Apr 24	4-	3-	3-	3+	3+	3	2+	3+	3+	3-	3-	2+	2	2-	3-	5+	3	2-	2-	3-	4	2+	3-	1	1-	5	3+	4-	3-	4+	
May 24	4-	7-	4	3	4+	5+	3-	2	2+	9-	9	7	6	2+	3	6	6	4	3-	2+	3-	2-	3+	3	2+	3-	3	2	2+	3+	4
Jun 24	2+	2+	4+	3-	2+	2	6+	5-	2	4	4	1+	1	2+	5-	4	3+	3+	3+	2+	1+	1+	3+	2-	3-	3-	3+	8-	4	4-	
Jul 24	2-	1+	1+	3	3	1	3-	3+	2+	2-	2	2	1+	1+	3	3+	2+	1+	1+	3-	2-	3	3-	2-	3+	5	4	3-	2	5+	5-
Aug 24	5+	3-	3-	7	3	2-	2+	3-	2	2+	5	8	4+	4-	2	3-	6+	4-	3	3+	3+	3	2+	3	2+	2-	3+	6-	2	5-	5-
Sep 24	4-	3-	2	4+	2-	3	2+	2+	3-	2+	4-	7	6	4+	4	4	7+	4-	4+	3+	2	2	4+	4+	5-	4	2+	3	4-	4	
Oct 24	2	2	3	3	2+	5-	6+	7	4+	9-	8+	5-	2-	4-	3+	3	3	4-	5	3	2	3	3	4+	1	4	3-	5-	4	4	4-
Nov 24	3-	4	4	4+	3-	3+	3	4-	Kp5	6-	3	2-	3-	4-	3+	3+	3-	2	3-	3-	3	3+	3-	4	3+	3	2+	2-	3-	4+	
Dec 24	3-	2+	3+	2	2+	2+	2-	2+	4+	2+	2	2+	2-	3+	3	4-	5+	4-	4-	4-	3+	3+	4-	3+	2	0+	1+	1+	2-	2+	4

Table 17: Kp values for year 2024

Considering the information reported in the Kp Matrix and considering that days having Kp values equal or below Kp 4 can be considered generally quiet days in term of solar storm, it is possible to create Table 18 containing for every day of the year both a Kp and G classification and a computation of the events having same G values during year 2024 as follows:

Kp Value	Classification	G Class	Events
Kp ≤ 4	No Storm	-	320
Kp = 5	Minor	G1	21
Kp = 6	Moderate	G2	10
Kp = 7	Strong	G3	7
Kp = 8	Severe	G4	4
Kp = 9	Extreme	G5	3

Table 18: G and Kp Values Matrix

4.2 Analysis of Doses and of Cumulative Yearly Dose

For the 2024 dose analysis, it was assumed that all events within the same G classification share uniform dose values across all scenarios. Without this assumption, the model would have required separate dose calculations for each day of the year.

Consequently, the dose for the "Deep-space daily dose" and "effective daily dose" previously calculated for the reference scenario and the five additional scenarios were then multiplied by the number of events associated with each specific scenario to obtain the Table 19:

Scenario	Day	G Class	Events	Deep-space Yearly Dose @400km (mSv)	Equivalent Yearly Dose @400km (mSv)
Reference	Dec 13th, 2024	-	320	310.080	226.304
Scenario 1	Aug 31st, 2024	G1	21	39.921	27.460
Scenario 2	May 17th, 2024	G2	10	28.850	19.961
Scenario 3	Aug 4th,2024	G3	7	22.841	15.554
Scenario 4	Mar 24th, 2024	G4	4	24.484	16.170
Scenario 5	May 10th, 2024	G5	3	88.920	62.094
2024 Yearly Dose				**515.096**	**367.543**

Table 19: Yearly Dose for Year 2024

The reference scenario, corresponding to the solar event of December 13th, 2024, produced the highest deep-space yearly dose of the dataset, with a value of 310.080 mSv. After applying shielding considerations, the equivalent yearly dose was reduced to 226.304 mSv. This event likely involved a significant solar particle enhancement and serves as the benchmark for evaluating all other scenarios during the year. The remaining five scenarios, each associated with geomagnetic disturbances classified under NOAA's G-scale (G1–G5), illustrate the substantial variability in radiation exposure driven by space-weather conditions.

The most intense of these, Scenario 5 (May 10th, 2024, G5), resulted in a deep-space dose of 88.920 mSv and an equivalent dose of 62.094 mSv, making it the second-highest contributor of the year. Despite shielding, this level of exposure highlights the elevated risk posed by extreme geomagnetic storms.

Scenario 4 (March 24th, 2024, G4) produced a deep-space dose of 24.484 mSv, slightly exceeding the 22.841 mSv recorded in Scenario 3 (August 4th, 2024, G3). This non-linear relationship between storm class and radiation dose reflects the complex dependence of exposure on particle spectra, event duration, and solar energetic particle characteristics.

Lower-intensity storms also contributed meaningfully to the yearly dose. Scenario 2 (May 17th, 2024, G2) resulted in 28.850 mSv deep-space dose and 19.961 mSv equivalent dose, while Scenario 1 (August 31st, 2024, G1) produced 39.921 mSv and 27.460 mSv, respectively. Although less severe than higher-class storms, these events still represent non-negligible contributions to cumulative astronaut exposure.

When aggregated, the total deep-space yearly dose from all recorded events in 2024 amounts to 515.096 mSv, with a cumulative equivalent dose of 367.543 mSv. While these values remain close to typical yearly radiation limits for astronauts, they underscore the operational importance of continuous radiation monitoring and adaptive shielding strategies during periods of heightened solar activity.

4.3 Exposure Time Limits and Mission Duration for Astronauts at LEO

The duration of radiation exposure in space is closely tied to the type and length of a mission. Short-term missions, such as those conducted during the Space Shuttle era, typically lasted from a few days to two weeks, with astronauts receiving total doses ranging from approximately 1 to 15 mSv (Cucinotta et al., 2001). These exposures correspond to average dose equivalent rates on the order of ~0.1 to 1 mSv/day, depending on mission duration and orbital parameters.

In contrast, long-duration missions aboard the International Space Station (ISS), which generally last between three and twelve months, result in significantly higher cumulative exposures. A typical six-month ISS mission leads to an accumulated dose of about 80 to 160 mSv, corresponding to average dose equivalent rates of approximately 0.4 to 0.8 mSv/day. These daily dose rates are strongly influenced by shielding effectiveness, orbital altitude and inclination, passages through the South Atlantic Anomaly, and modulation of galactic cosmic rays by the solar cycle (Berger, 2008; Zeitlin et al., 2013).

A recent study by Matthiä et al. (2024) reported nearly 13 years of continuous dose-equivalent measurements from the two DOSTEL instruments inside the Columbus laboratory on the ISS. Spanning solar cycle 24 and the early rise of cycle 25, the dataset provides a rare long-term record of the low Earth orbit radiation environment and its modulation by solar activity.

Across the 2009–2022 interval, the mean quality factor was 3.19 ± 0.12 for GCRs, while radiation-belt particles encountered mainly in the South Atlantic Anomaly showed a lower value of 1.24 ± 0.24. Correspondingly, total dose-equivalent rates inside Columbus ranged from about 0.5 mSv/day in 2015 to roughly 0.8 mSv/day in 2021. Solar cycle effects were clearly reflected in the GCR-driven component. During the 2014 solar maximum, when GCR intensities reached their minimum, the orbit-averaged dose-equivalent rate was 0.40 ± 0.02 mSv/day. During the 2020 solar minimum, when GCR fluxes peaked, the rate increased to 0.51 ± 0.02 mSv/day, with statistical uncertainties below 1%.

To approximate conditions outside Earth's magnetic shielding, measurements were further restricted to regions with geomagnetic cut-off rigidity below 0.5 GV and corrected for Earth shadowing. Under these effectively deep-space conditions, dose-equivalent rates reached 1.13 ± 0.04 mSv/day during the 2014 solar maximum and rose to 1.85 ± 0.07 mSv/day during the 2020 solar minimum.

The six-month mission duration was established early in the ISS program as a strategic compromise, balancing scientific return with the need to manage the physiological and psychological challenges posed by microgravity, isolation, and radiation exposure. This time frame also aligns with the logistical cadence of crewed transport vehicles such as Soyuz, Crew Dragon, and CST-100 Starliner. Crew rotations are typically staggered to ensure continuous human presence aboard the ISS, which supports operational safety and uninterrupted scientific experimentation.

While six months remains the standard mission length, several longer-duration missions have been undertaken to investigate the effects of extended exposure to space conditions. A notable example is the 340-day mission completed in 2015–2016 by NASA astronaut Scott Kelly and Russian cosmonaut Mikhail Kornienko. This mission provided critical biomedical data for planning future deep space exploration, including potential missions to Mars (Garrett-Bernardin et al., 2019).

To mitigate health risks, space agencies implement stringent radiation dose limits as indicated in Table 19. NASA establishes career dose thresholds to ensure that the risk of radiation-induced cancer mortality (REID) remains below 3%. Following the 2022 revision of NASA-STD-3001, this threshold was standardized to a universal limit of 600 mSv for the entire astronaut career, replacing the previous age- and sex-dependent model (Simonsen et al., 2020; National Academies of Sciences, Engineering, and Medicine, 2021).

5. Discussion

5.1 Values Comparison

Annual Comparison with Regulatory Limits

By comparing the yearly deep-space dose rate to internationally recognized dose limit, it becomes possible to develop altitude-specific safety protocols. These measures, summarized in the Table 20, are essential for maintaining occupational exposures within acceptable thresholds and supporting the continued advancement of aviation and space operations.

	Deep Space Dose (mSv/year)	Equivalent Dose (mSv/year)
2024 Yearly Dose Rate	515.096	367.543
Career Limit Dose Rate	600	600
Difference	−14.15 %	−38.74 %

Table 20: Yearly Dose Rate Table Comparison

In 2024, the deep space yearly dose rate reached 515.096 mSv, remaining 14.15 % below the commonly adopted career limit of 600 mSv. This indicates that, in the absence of shielding, the radiation environment in low Earth orbit (LEO) approached levels of operational concern during the year but did not exceed long-term exposure constraints. After accounting for standard spacecraft shielding, the equivalent yearly dose rate was reduced to 367.543 mSv, which is 38.74 % below the same career limit. Although this value remains well within accepted exposure constraints, it still represents a substantial fraction of the allowable cumulative dose and leaves limited margin for additional contributions from transient events such as solar particle events or prolonged operations in regions of enhanced trapped radiation.

Space agencies, including NASA and ESA, apply conservative radiation exposure limits to mitigate long-term health risks such as carcinogenesis, cardiovascular degradation, and central nervous system effects (Cucinotta & Chappell, 2011). The proximity of the 2024 equivalent dose rate to the regulatory threshold underscores the sensitivity of astronaut exposure to variations in shielding performance, orbital inclination, altitude, and space-weather conditions.

The elevated dose rates observed in 2024 are consistent with the increasing solar activity associated with the ascent toward the Solar Cycle 25 maximum, during which enhanced solar and geomagnetic disturbances can significantly intensify the radiation environment in LEO (Reames, 2013). These findings highlight the importance of continuous radiation monitoring, robust shielding strategies, and adaptive mission planning to ensure compliance with radiation protection standards—particularly during periods of heightened solar activity and for future long-duration missions in LEO and beyond (Durante & Cucinotta, 2011; Hellweg & Baumstark-Khan, 2007).

Comparison with established literature

Following the full-year analysis, the simulated radiation environment was compared against representative values reported in the literature. All references were consistently normalised to annual doses under solar-minimum conditions, during which galactic cosmic ray (GCR) fluxes reach their maximum, providing the most conservative and directly comparable baseline. The comparison is summarised in Table 21.

	Deep Space Dose (mSv/year)	Equivalent Dose (mSv/year)
Simulation Results	515	368
NASA/MSFC (2017)	-	320
Hodkinson at al. (2017)	-	310
Matthiä et al (2024)	676	292

Table 21: Yearly Equivalent Dose Table Comparison

The simulation yields an annual deep-space dose of approximately 515 mSv/year and an equivalent dose of approximately 368 mSv/ year at 400 km altitude. Both values fall within the range reported by contemporary experimental and modelling studies, supporting the validity of the simulated radiation environment.

The most direct comparison is with Matthiä et al. (2024), who reported a deep-space dose of 676 mSv/ year and an equivalent dose of 292 mSv/ year during the 2020 solar minimum. The present simulation produces a deep-space dose roughly 23% lower and an equivalent dose roughly 26% higher. This inverse relationship likely reflects differences in the GCR spectrum model and dose-conversion methodology applied, particularly in the assumed particle species composition and biological quality factors. The earlier estimates from NASA/MSFC (2017) and Hodkinson et al. (2017), at 320 mSv/ year and 310 mSv/ year respectively, sit between the present result and the Matthiä et al. (2024) value, indicating a systematic rather than anomalous spread across studies. The present simulation lies closest to the NASA/MSFC (2017) estimate, with a difference of approximately 15%.

Overall, agreement across all four datasets falls within a factor of approximately 1.3, which is considered acceptable in radiation modelling given the inherent variability of the space environment and the fact that each reference reflects different instruments, orbital parameters, and modelling assumptions.

To further validate the simulation on a shorter timescale, the daily equivalent dose was compared against literature-derived daily rates. The comparison is summarised in figure 8:

	Daily Equivalent Dose (mSv/d)
Simulation Results	1.007
NASA/MSFC (2017)	0.877
Hodkinson at al. (2017)	0.849

Matthiä et al (2024)	0.800

Table 22: Daily Equivalent Dose Table Comparison

Figure 8: Daily Equivalent Dose Comparison

The simulation yields a daily equivalent dose of approximately 1.007 mSv/day, representing the upper bound across the comparison set. The literature-derived daily rates, obtained by normalising the annual estimates from NASA/MSFC (2017), Hodkinson et al. (2017), and Matthiä et al. (2024), range from 0.800 to 0.877 mSv/day, placing the simulation approximately 15% to 26% above these values, consistent with the trend already observed in the annual comparison. The spread across all four values falls within a factor of approximately 1.3, which is considered well within the accepted range for space radiation modelling.

The observed offset is fully consistent with the methodology employed and reflects the inherent characteristics of the simplified analytical scaling model adopted in this study. By estimating dose rates through parameterised relationships between radiation intensity, altitude-dependent transmission, and exposure duration, the model prioritises physical transparency and computational efficiency over instrument-specific replication. Reference values from the literature are derived from fixed detector measurements aboard specific spacecraft or high-fidelity transport codes calibrated to particular mission profiles, each embedding its own assumptions regarding shielding geometry, GCR spectral input, and biological quality factors. The fact that the simulation result falls consistently above the reference values demonstrates a coherent and physically interpretable behaviour, confirming that the model responds predictably to its inputs. Overall, the agreement across all four datasets is considered satisfactory, and the results provide a reliable and physically grounded estimate of the daily radiation environment at 400 km altitude.

Methodology Consideration

The methodological framework adopted in this study represents a systematic and computationally efficient approach to annual radiation dose assessment that effectively balances physical accuracy with practical feasibility. The core strength of this methodology lies in its strategic simplification of complex space weather phenomena while preserving the essential physics governing radiation exposure during geomagnetic disturbances.

Central to this approach is the temporal aggregation of geomagnetic events according to NOAA G-classification (G0–G5). Rather than performing computationally prohibitive day-by-day dose calculations throughout 2024, all geomagnetic disturbances within each storm class were assigned identical dose contributions derived from representative simulated scenarios. This classification-based aggregation significantly reduces computational demands while maintaining critical sensitivity to storm severity, the primary driver of radiation enhancement. Although this method intentionally abstracts intra-class variability in storm duration, spectral characteristics, and temporal evolution, it provides a conservative and tractable framework for estimating cumulative annual dose that captures the dominant physical effects.

The shielding model employed further demonstrates the methodological rigor of this work. Mean percentage shielding factors, ranging from approximately 39% to 49% depending on storm intensity, were derived from systematic comparisons between external and internal dose rates in the Zvezda module (Table 8). Importantly, the methodology explicitly accounts for the dynamic nature of shielding effectiveness by incorporating storm-class-dependent variations in shielding performance relative to quiet conditions. This storm-responsive shielding model represents a significant advancement over constant-shielding assumptions. The extension of Zvezda-derived shielding characteristics to all pressurized ISS modules is justified by their comparable areal densities and structural designs, with the acknowledged caveat that localized material and equipment variations constitute second-order effects compared to the primary storm-driven radiation enhancements captured by the model.

The validity and practical utility of this methodology are underscored by the consistency of results with independent measurements and advanced modeling efforts incorporating deep-space-adjusted radiation environments and enhanced space-weather resolution. While numerical differences between approaches may appear modest, this convergence across methodologies with different underlying assumptions strengthens confidence in the dose estimates and confirms their suitability for operational radiation protection planning. The methodology successfully achieves its dual objectives: providing physically realistic dose assessments that respond appropriately to both geomagnetic storm severity and shielding variations, while remaining computationally feasible for routine application. For radiation protection purposes, the ability to efficiently evaluate annual dose

accumulation across the full spectrum of space weather conditions represents a significant practical advantage, enabling timely risk assessments and mission planning decisions without sacrificing essential physical fidelity.

5.2 Mitigations strategies

Radiation exposure in Low Earth Orbit (LEO) remains a significant concern for astronaut health, despite partial shielding by Earth's magnetosphere. Aboard the International Space Station (ISS), astronauts are continuously exposed to galactic cosmic rays (GCRs) and, intermittently, to solar particle events (SPEs). These ionizing radiation sources contribute to elevated long-term health risks, including cancer, cardiovascular disease, and neurodegenerative conditions.

Galactic cosmic rays (GCRs) represent a continuous background radiation source that exhibits relatively stable, predictable variations over time. Unlike the sporadic and intense bursts of solar energetic particles, GCR intensity follows a regular pattern tied to the approximately 11-year solar cycle. This relationship is clearly demonstrated by neutron monitor data—ground-based instruments that indirectly measure cosmic ray activity by detecting secondary particles produced when cosmic rays enter Earth's atmosphere.

The monthly neutron count data in Figure 9 from the Oulu Neutron Monitor in Finland, spanning from 1964 to 2025, reveals a consistent and predictable pattern: cosmic ray intensity increases during solar minimum periods (when the Sun is quiet) and decreases during solar maximum periods (when the Sun is most active). This inverse relationship occurs because the Sun's magnetic field and solar wind act as a shield that deflects incoming cosmic rays. When solar activity is high, this shield is stronger, blocking more cosmic rays from reaching Earth and the ISS. Conversely, during solar minimum, the weakened shield allows more cosmic rays to penetrate.

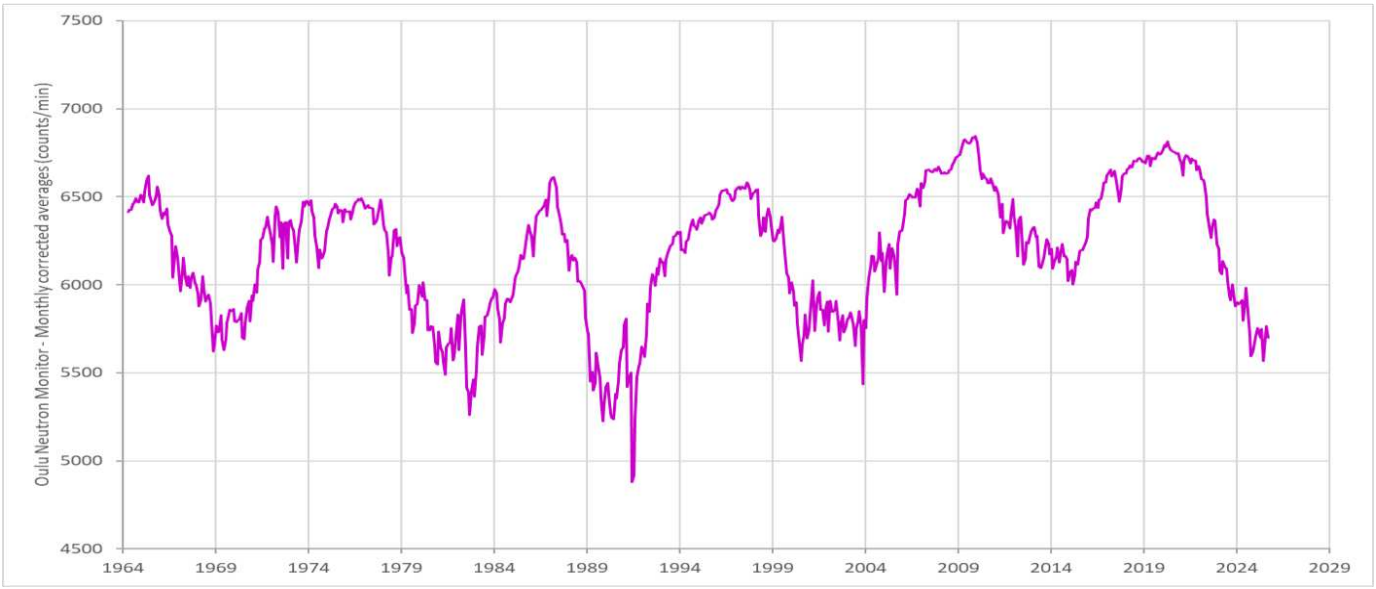


Figure 9: Neutron Monitoring from 1964 to 2025 (STCE Cosmic Rays, 2025)

As Figure 8 illustrates, over six decades of observation, GCR levels have typically varied by about 15–20% above and below the long-term average. The most recent peak occurred in late 2020 and early 2021, corresponding to the deep solar minimum between Solar Cycles 24 and 25. This was followed by a decline of approximately 10% as Solar Cycle 25 began ramping up, demonstrating the expected inverse relationship between solar activity and cosmic ray intensity.

For astronauts aboard the International Space Station, these GCR variations have direct practical implications. Although the ISS orbits within low Earth orbit (LEO), it flies above most of Earth's protective atmosphere, placing crews in a radiation environment that responds to solar cycle changes. During solar minimum periods, such as 2019–2020, ISS radiation measurements consistently show elevated dose rates from cosmic rays. During solar maximum periods, the strengthened solar magnetic field suppresses cosmic ray intensity, providing some natural relief from this constant radiation background. ISS missions conducted during the early phase of Solar Cycle 25 (2021–2023) therefore experienced lower GCR dose rates compared to the preceding solar minimum.

However, it is important to recognize that these conditions represent only one phase of the solar cycle and should not be considered typical of all mission scenarios. As Solar Cycle 25 continues toward its maximum (expected around 2025–2026), GCR levels will remain relatively low. Subsequently, as solar activity declines toward the next minimum (around 2030), GCR intensity will gradually rise again, eventually returning to levels comparable to those observed in 2019–2020. The practical implication for mission planning is clear: the timing of ISS missions within the solar cycle significantly influences crew radiation exposure from cosmic rays. Missions during solar minimum face higher continuous GCR dose rates, while missions during solar maximum benefit from reduced GCR exposure, though this advantage is partially offset by the increased risk of intense solar particle events during active solar periods. Understanding this predictable cycle allows mission planners to better assess radiation risks and implement appropriate protective measures based on when missions are scheduled relative to solar activity levels.
Within this framework, Solar Energetic Particle (SEP) events constitute a particularly critical and unpredictable radiation hazard due to their sporadic occurrence, extreme variability, and potentially life-threatening intensity. Unlike the more gradual and predictable variations associated with geomagnetic storms, SEP events are inherently intermittent phenomena that can emerge suddenly during periods of intense solar activity, creating acute radiation exposures that pose immediate dangers to astronaut health. The unpredictable timing and magnitude of these events represent one of the most challenging aspects of space radiation protection, as illustrated in Figure 10, which documents the highly irregular pattern of SPE activity from 1976 to 2025.

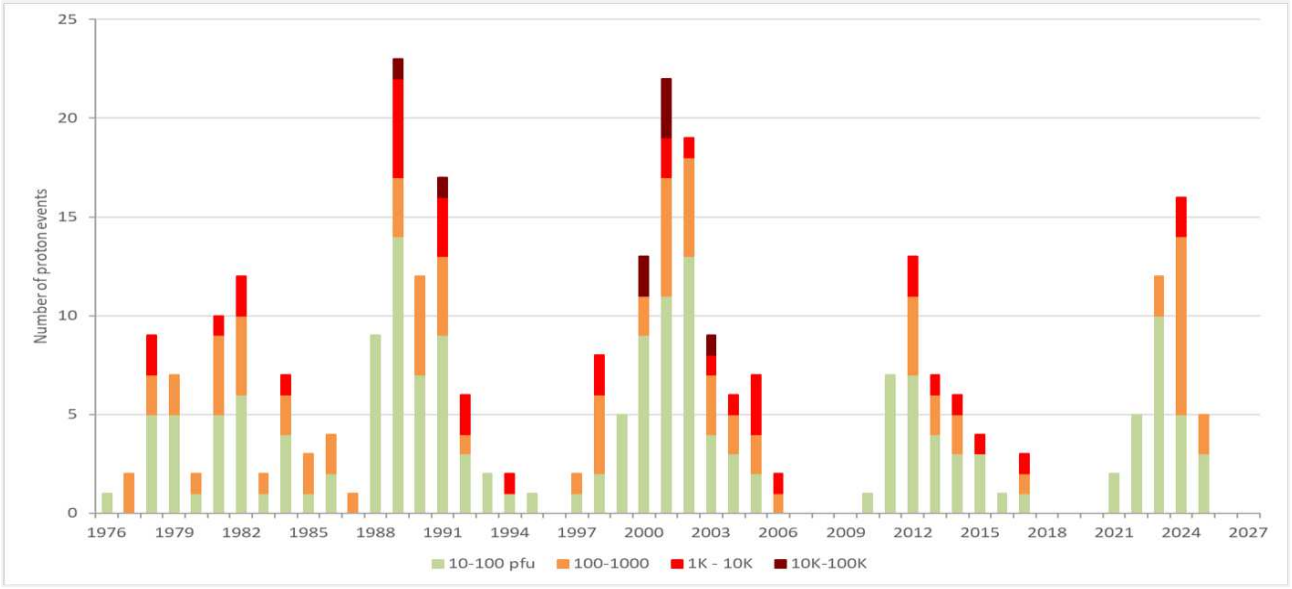


Figure 10: Proton Events from 1976 to 2025 (STCE Protons, 2025)

Figure 9 reveals the fundamentally non-constant and episodic nature of the SEP radiation environment. The characteristic 11-year solar cycle periodicity is evident, with pronounced activity maxima around 1990, 2001, and 2013, and renewed intensification from 2023 onward. However, within these cycles, the distribution of events is highly irregular and unpredictable. While the majority of proton events exhibit relatively modest fluxes in the 10–100 pfu range, the most hazardous characteristic of SEP activity is the sporadic occurrence of extreme episodes that can suddenly escalate beyond 1,000 pfu with little warning. These high-intensity events are not merely statistical outliers; they represent genuine emergencies capable of delivering radiation doses in hours that would otherwise accumulate over weeks or months during quiet conditions.

The intermittent and unpredictable nature of SEP events creates a fundamentally different risk profile compared to chronic radiation exposures. During these sporadic but intense episodes, astronauts face acute radiation exposure scenarios that can rapidly approach or exceed safe operational limits, potentially causing immediate radiation sickness, increasing cancer risk, and threatening mission success. The danger is compounded by the fact that SEPs can penetrate spacecraft shielding more effectively than trapped radiation belt particles, and their occurrence cannot be reliably predicted more than minutes to hours in advance. This combination of high intensity, sporadic occurrence, limited predictability, and direct health consequences makes SEP events one of the most serious and operationally challenging radiation hazards for human spaceflight. The variability shown in Figure 9 underscores that crew radiation exposure during solar maximum periods is not simply elevated—it is fundamentally uncertain, with the ever-present possibility of sudden, extreme events that demand immediate protective action and can severely constrain mission operations or even necessitate mission abort scenarios.

For these reasons, it is fundamental to have an effective risk management based on an integrated framework that combines predictive science, operational planning, and engineering solutions.

A) Predictive Science: Forecasting and early-warning systems

Forecasting and early-warning systems provide mission controllers with the temporal awareness needed to anticipate solar disturbances and act before radiation levels spike.

Specifically, forecasting being a probabilistic, planning-oriented activity that integrates solar observations, heliospheric modelling, and historical statistics estimates the timing and likelihood of solar wind disturbances and coronal mass ejections (CMEs). These systems, such as NASA's Space Weather Prediction Center (SWPC), NOAA's GOES satellite constellation, and ESA's SEPEM model, track solar activity and model the propagation of solar energetic particles (SEPs) and coronal mass ejections (CMEs) from the Sun toward Earth (Reames, 2013). By analyzing real-time satellite data and solar observations, these forecasting tools can predict an increase in radiation levels hours or even days in advance. Forecasting systems play a crucial operational role by providing astronauts and mission planners with the information needed to avoid or minimize exposure during high-radiation events. For example, if a strong solar flare or CME is predicted to impact LEO, mission control can issue alerts that prompt astronauts to suspend extravehicular activities (EVAs), delay sensitive operations, or move to better-shielded parts of the spacecraft. These protocols significantly reduce the dose astronauts would otherwise receive. Moreover, predictive tools allow for real-time coordination between space weather centers and crewed missions, ensuring timely protective actions such as shelter-in-place procedures (Camporeale, 2019).

Early-warning systems provide immediacy through low-latency in situ measurements of solar wind and energetic particles. Particle detectors and dosimeters translate rising fluxes into automated alerts linked to predefined protective actions. Radiation detectors aboard spacecraft such as the International Space Station (ISS) provide continuous monitoring of the radiation environment. These instruments include dosimeters, spectrometers, and tissue-equivalent proportional counters (TEPCs), each of which contributes to measuring different aspects of the radiation field. For instance, the Radiation Assessment Detector (RAD) and the Passive Dosimeter for Life Science Experiments in Space (PADLES) are used to quantify radiation doses from galactic cosmic rays (GCRs) and solar particle events (SPEs) (Zeitlin et al., 2013). These detectors are positioned in various locations throughout the spacecraft, offering spatial resolution that informs risk-based decisions such as where astronauts should sleep, work, or take shelter. Among the most critical tools are tissue-equivalent detectors, which simulate human biological tissue to provide a biologically relevant measurement of radiation dose. The data gathered are used to estimate equivalent dose and assess potential health impacts, supporting risk modeling and compliance with dose limits set by international spaceflight guidelines

Although forecasting and early warning rely on distinct methodologies (ensemble heliospheric modelling versus deterministic, threshold-based detection) they serve complementary roles. Forecasting supports strategic planning and minimizes unnecessary constraints, while early warning mitigates acute exposure during rapid solar energetic particle events. Their integration is essential for effective radiation-risk management in LEO missions.

B) Operational Planning: Mission Planning

Space weather introduces hazards that fundamentally shape the design, scheduling, and operations of human missions beyond Earth. Mission planners must integrate mitigation strategies to protect both crews and spacecraft electronics outside the shield of Earth's magnetosphere. These risks directly determine mission structure, crew duration in deep space, and the prioritization of daily operations (Cucinotta et al., 2014).

Galactic cosmic rays (GCRs) present a persistent challenge. These high-energy particles are ever-present in interplanetary space and continuously accumulate dose. Unlike other hazards, GCR exposure cannot be reduced through real-time actions, forcing designers to embed constraints into mission architecture. The most consequential outcome is a limit on total mission duration: astronauts' lifetime exposure must remain within medical thresholds, meaning GCRs set a ceiling on how long crews can safely operate in deep space (Durante, 2014; Cucinotta et al., 2006). Thus, GCRs influence both spacecraft design and the fundamental timeline of exploration.

Solar energetic particles (SEPs), by contrast, pose acute and intermittent threats. SEP events can raise dose rates by orders of magnitude within minutes to hours, requiring immediate response. Protocols mandate rapid crew relocation to storm shelters, superseding all other activities. This ability to suspend operations and prioritize protection reflects the unpredictable and potentially severe nature of SEP events (Papaioannou et al., 2022).

The dual nature of radiation hazards, persistent GCRs and sporadic SEPs, requires balancing long-term constraints with short-term contingencies. GCRs impose structural and temporal limits, while SEPs demand flexible, rapid responses that can override all other priorities. Together, they create a complex environment in which engineering, crew safety, and mission objectives must be continuously harmonized (Carnell, 2020; Spillantini et al., 2007; Washburn et al., 2015). In essence, space mission planning is defined by this interplay: managing the slow accumulation of GCR dose over months while preparing for the sudden onset of SEP events. Success depends on integrating these realities into every aspect of design and operations, ensuring astronauts can explore interplanetary space with both safety and effectiveness preserved (Cheraghi et al., 2021).

By applying this operational strategy, is it possible to compare the previously calculated equivalent dose for the year 2024 to a six-month mission scenario and evaluate the mitigation effects as indicated in Table 23:

	Deep Space Dose (mSv/year)	Equivalent Dose (mSv/year)
2024 Semesterly Dose Rate	**257.548**	**183.771**
Career Limit Dose Rate	**600**	**600**
Difference	**−57.09 %**	**−69.37 %**

Table 23: Semesterly Dose Rate Table Comparison

The semesterly deep-space dose is estimated at 257.548 mSv, corresponding to a value 57.09 % below the annual regulatory limit. This indicates that, over a six-month exposure period, the deep-space radiation environment in low Earth orbit (LEO) remains within acceptable regulatory bounds. Similarly, the semesterly equivalent dose is estimated at 183.771 mSv, which is 69.37 % below the annual limit. This further confirms that, under the modelled conditions, crew exposure during a six-month mission at 400 km altitude remains well below the regulatory threshold. Overall, these results provide additional confidence that the simulated radiation environment is consistent with current operational limits for human spaceflight in LEO.

C) **Engineering Solutions:** Shielding strategies

Shielding strategies, form the physical foundation of radiation defence in space, requiring a balance between radiological effectiveness, structural constraints, and operational feasibility to limit astronaut exposure in spacecraft. When shielding and other mitigating factors are considered, the equivalent semesterly dose is further reduced to 229.42 mSv, corresponding to 54.12% below the annual regulatory limit. This substantial reduction highlights the effectiveness of shielding and operational mitigation strategies in limiting radiation exposure for orbital missions. Figure 10 illustrates the comparison between the deep space and deep space semesterly dose rates relative to the 600 mSv regulatory limit, clearly showing that both exposure scenarios remain below the prescribed threshold for the analysed period.

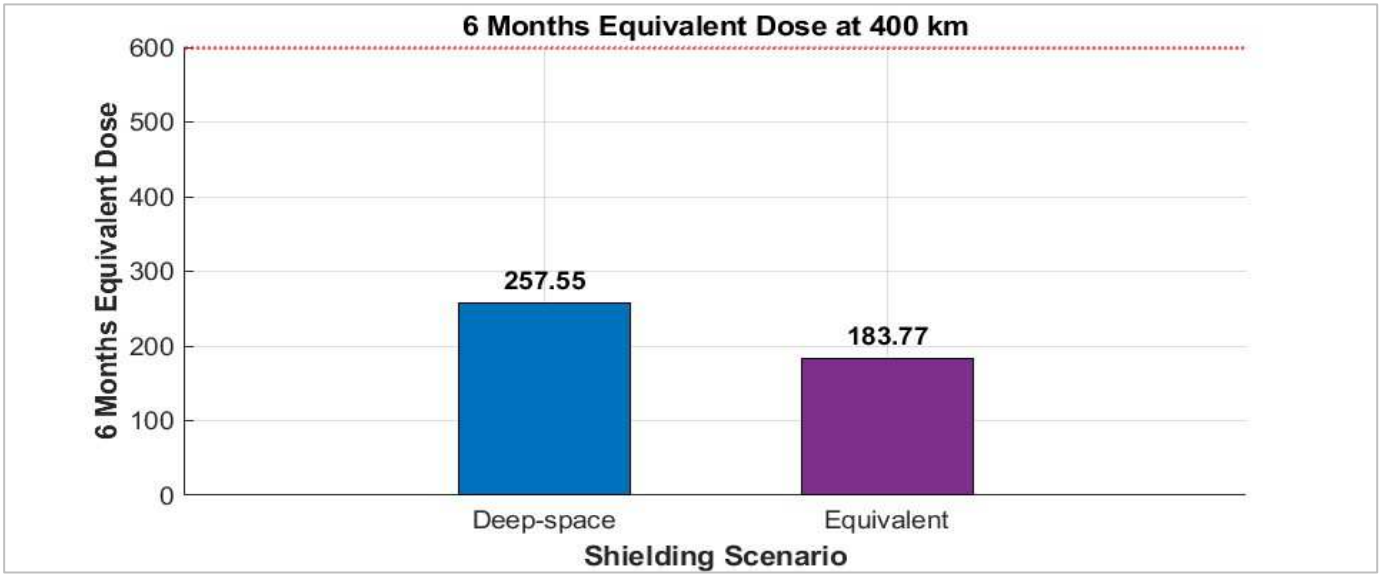


Figure 11: Deep Space and Equivalent 6 Months Dose Rate Comparison

The results indicate that adequate shielding on board spacecraft plays a vital role in significantly reducing radiation exposure, ensuring that the equivalent dose remains within acceptable safety limits for a standard six-month mission in low Earth orbit (LEO). These findings highlight the essential function of both physical shielding and well-designed operational protocols in mitigating the health risks posed by space radiation. In scenarios without shielding, the projected radiation dose exceeds established regulatory limits, demonstrating the necessity of protective measures. However, under more realistic mission conditions that include proper shielding, astronaut's exposure can be maintained at levels considered safe for the typical mission duration. This evidence supports the current practice of limiting mission length to approximately six months, as extending the duration would lead to higher cumulative radiation doses. Even with shielding, prolonged exposure could exceed permissible thresholds, posing increased health risks to crew members. Therefore, both mission planning and spacecraft design must prioritize radiation protection to ensure astronaut safety during extended spaceflight

In conclusion, these three complementary approaches constitute the pillars of radiation protection for LEO missions. Forecasting and early warning address the challenge of probabilistic anticipation, allowing crews to prepare for threats before they materialize. Mission planning enables operational adaptation, reshaping activities and schedules to minimize exposure when conditions deteriorate. Shielding provides physical attenuation, reducing the intensity of radiation that reaches crew members through carefully designed barriers and refuge areas. Each addresses a different dimension of the radiation challenge, and their integration is essential to safeguarding astronauts and ensuring the viability of long-duration exploration beyond low Earth orbit.

6. Conclusion

In summary, radiation exposure remains the preeminent health challenge for crew members operating in Low Earth Orbit (LEO), where the Earth's magnetosphere provides only partial protection against energetic particle fluxes. The findings of this study confirm that annual equivalent doses remain consistent with contemporary measurements, yet they underscore a critical paradigm shift in how radiation risk assessment must be approached within dynamic orbital environments.

A central contribution of this research is demonstrating that computationally intensive simulations can be effectively complemented by streamlined analytical methodologies. While traditional methods remain indispensable for high-fidelity modelling, their substantial computational resource requirements often preclude the operational agility necessary for rapid decision-making in real-time scenarios. By introducing a validated scaling model, derived from and corroborated against empirical datasets, this study demonstrates that near-instantaneous dose estimations can be achieved with minimal deviation from those produced by more rigorous, computationally demanding frameworks, ensuring that computational expediency does not compromise operational safety.

Ultimately, this methodology represents a balance between physical realism and computational tractability. The integrated framework, which maintains high sensitivity to both geomagnetic storm intensity and spacecraft shielding efficacy, enables a more proactive risk mitigation strategy. By synthesizing real-time environmental monitoring with advanced forecasting capabilities, mission controllers can more effectively schedule Extravehicular Activities (EVAs) and optimize the deployment of hardened storm shelters during periods of solar activity. This approach not only enhances the operational resilience of current ISS missions but also provides a scalable blueprint for the next generation of long-duration deep-space exploration endeavours.

Declarations

No funding was received for conducting this study.
The author has no financial or proprietary interests in any material discussed in this article.
The author has no competing interests to declare that are relevant to the content of this article.
Author and co-authors contributed to the research and have commented, edited, and reviewed the manuscript.
Author and co-authors read and approved the final manuscript.

Data availability

The data supporting the findings of this study are public or available within the paper. Supplementary information is available from the authors on reasonable request.

Orcid

Alessandro Bucci. https://orcid.org/0009-001-0205-4585

References

Barger, L. K., Flynn-Evans, E. E., Kubey, A., Walsh, L., Ronda, J. M., Wang, W., ... & Czeisler, C. A. (2014). Prevalence of sleep deficiency and use of hypnotic drugs in astronauts before, during, and after spaceflight: An observational study. *The Lancet Neurology, 13*(9), 904–912. https://doi.org/10.1016/S1474-4422(14)70122-X

Barratt, M. R., & Pool, S. L. (Eds.). (2008). *Principles of clinical medicine for space flight*. Springer.

Berger, T. (2008). Radiation dosimetry onboard the International Space Station (ISS). Zeitschrift für Medizinische Physik, 18(4), 265–275. https://doi.org/10.1016/j.zemedi.2008.06.014

Bucci, A., Romito, A., Aspetti, P. C., Mucciarelli, L., & Malizia, A. (2025). *Impact of space weather on higher airspace operations and commercial space operations*.

Burrell, M. O., Wright, J. J., & Watts, J. W. (1968). *An analysis of energetic space radiation and dose rates* (NASA-TN-D-4529). Washington, DC: NASA.

Camporeale, E. (2019). The challenge of machine learning in space weather: Nowcasting and forecasting. *Space Weather, 17*(8), 1166–1207. https://doi.org/10.1029/2018SW002061

Carnell, L. S. (2020). Spaceflight medical countermeasures: A strategic approach for mitigating effects from solar particle events. *International Journal of Radiation Biology, 97*(sup1), S125–S131. https://doi.org/10.1080/09553002.2020.1820603

Cheraghi, E., Chen, S., & Yeow, J. T. W. (2021). Boron nitride-based nanomaterials for radiation shielding: A review. *IEEE Nanotechnology Magazine, 15.* https://doi.org/10.1109/MNANO.2021.3066390

Cucinotta, F. A., & Chappell, L. J. (2011). *Space radiation cancer risk projections and uncertainties—2010* (NASA Technical Paper 2011-216155). NASA. https://ntrs.nasa.gov/citations/20110015800

Cucinotta, F. A., & Durante, M. (2006). Cancer risk from exposure to galactic cosmic rays: Implications for space exploration by human beings. *The Lancet Oncology, 7*(5), 431–435. https://doi.org/10.1016/S1470-2045(06)70695-7

Cucinotta, F. A., Kim, M. Y., Chappell, L. J., & Huff, J. L. (2014). How safe is safe enough? Radiation risk for a human mission to Mars. *PLoS ONE, 8*(10), e74988. https://doi.org/10.1371/journal.pone.0074988

Cucinotta, F. A., Kim, M.-H. Y., & Ren, L. (2006). Evaluating shielding effectiveness for reducing space radiation cancer risks. Radiation Measurements, 41(9–10), 1173–1185. https://doi.org/10.1016/j.radmeas.2006.03.011

Cucinotta, F. A., Schimmerling, W., Wilson, J. W., Peterson, L. E., Badhwar, G. D., Saganti, P. B., & Dicello, J. F. (2001). *Space radiation cancer risks and uncertainties for Mars missions*. Radiation Research, 156(5), 682–688. https://doi.org/10.1667/0033-7587(2001)156[0682:SRCRAU]2.0.CO;2

Durante, M. (2014). Space radiation protection: Destination Mars. Life Sciences in Space Research, 1, 2–9. https://doi.org/10.1016/j.lssr.2014.01.002

Durante, M., & Cucinotta, F. A. (2011). Physical basis of radiation protection in space travel. *Reviews of Modern Physics, 83*(4), 1245–1281. https://doi.org/10.1103/RevModPhys.83.1245

Dyer, C., Lei, F., Clucas, S., Smart, D. F., & Shea, M. A. (2003). Calculations and observations of solar particle enhancements to the radiation environment at aircraft altitudes. *Advances in Space Research, 32*(1), 81–93. https://doi.org/10.1016/s0273-1177(03)90374-7

Garrett-Bernardin, L. G., Bailey, S., Cekanaviciute, E., Chouker, A., Cruz-Hernández, P., da Silva López, E., … & Zwart, S. R. (2019). The NASA Twins Study: A multidimensional analysis of a year-long human spaceflight. *Science, 364*(6436), eaau8650. https://doi.org/10.1126/science.aau8650

Ginet, G. P., O'Brien, T. P., Huston, S. L., Johnston, W. R., Guild, T. B., Friedel, R. H. W., ... & Whelan, P. (2013). AE9, AP9 and SPM: New models for specifying the trapped energetic particle and space plasma environment. *Space Science Reviews, 179*(1–4), 579–615. https://doi.org/10.1007/s11214-013-9964-y

Hellweg, C. E., & Baumstark-Khan, C. (2007). Getting ready for the manned mission to Mars: The astronauts' risk from space radiation. *Naturwissenschaften, 94*(7), 517–526. https://doi.org/10.1007/s00114-006-0204-0

Hodkinson, P. D., Anderton, R. A., Posselt, B. N., & Fong, K. J. (2017). *An overview of space medicine*. *British Journal of Anaesthesia, 119*(Suppl. 1), i143–i153. https://doi.org/10.1093/bja/aex336

Larsen, N. (2023). Radiation impact of GLE 73. PoS(ICRC2023), 1261. https://doi.org/10.22323/1.444.1261

Matthiä, D., Burmeister, S., Przybyla, B., & Berger, T. (2024). *Active radiation measurements over one solar cycle with two DOSTEL instruments in the Columbus laboratory of the International Space Station*. Life Sciences in Space Research, 38, 1–12. https://doi.org/10.1016/j.lssr.2023.04.002

NASA (2025). https://www.nasa.gov/international-space-station/space-station-facts-and-figures/

NASA. (2020). *NASA astronaut training manual: EVA operations*.

NASA/MSFC. (2017). Space faring: The radiation challenge (EP–2008–08–116-MSFC) [PDF]. National Aeronautics and Space Administration. https://www.nasa.gov/wp-content/uploads/2017/04/radiationchallenge.pdf?emrc=ba69fbin

National Academies of Sciences, Engineering, and Medicine. (2021). Space radiation and astronaut health: Managing and communicating cancer risks. The National Academies Press. https://doi.org/10.17226/26155

National Research Council. (2008). *Managing space radiation risk in the new era of space exploration*. The National Academies Press. https://doi.org/10.17226/12045

Papaioannou, A., Vainio, R., Raukunen, O., Jiggens, P., Aran, A., Dierckxsens, M., … Anastasiadis, A. (2022). *The Probabilistic Solar Particle Event foRecasting (PROSPER) model: Forecasting SEP event probability and peak flux.* arXiv. https://arxiv.org/abs/2205.07325

Reames, D. V. (2013). The two sources of solar energetic particles. *Space Science Reviews, 175*(1–4), 53–92. https://doi.org/10.1007/s11214-013-9958-9

Sato, T., Niita, K., Shurshakov, V. A., Yarmanova, E. N., Nikolaev, I. V., Iwase, H., Sihver, L., Mancusi, D., Endo, A., Matsuda, N., Iwamoto, Y., Nakashima, H., Sakamoto, Y., Yasuda, H., Takada, M., & Nakamura, T. (2011). Evaluation of dose rate reduction in a spacecraft compartment due to additional water shield. *Cosmic Research, 49*(4), 319–324. https://doi.org/10.1134/S0010952511040083

Simonsen, L. C., Nealy, J. E., Townsend, L. W., & Wilson, J. W. (1990). Space radiation shielding for a Martian habitat. *SAE Technical Paper Series*, Paper 901346. https://doi.org/10.4271/901346

Simonsen, L. C., Slaba, T. C., Guida, P., & Rusek, A. (2020). NASA's first ground-based Galactic Cosmic Ray simulator: Enabling a new era in space radiobiology research. *PLOS Biology, 18*(5), e3000669. https://doi.org/10.1371/journal.pbio.3000669

Space Weather Live 2024/03/24. https://www.spaceweatherlive.com/en/archive/2024/03/24.html

Space Weather Live 2024/05/10. https://www.spaceweatherlive.com/en/archive/2024/05/10/dayobs.html

Space Weather Live 2024/05/17. https://www.spaceweatherlive.com/en/archive/2024/05/17.html

Space Weather Live 2024/08/04. https://www.spaceweatherlive.com/en/archive/2024/08/04/dayobs.html
Space Weather Live 2024/08/31. https://www.spaceweatherlive.com/en/archive/2024/08/31.html
Space Weather Live 2024/12/13. https://www.spaceweatherlive.com/en/archive/2024/12/13/dayobs.html
Spillantini, P., Casolino, M., Durante, M., Mueller-Mellin, R., Reitz, G., Rossi, L., Shurshakov, V., & Sorbi, M. (2007). Shielding from cosmic radiation for interplanetary missions: Active and passive methods. *Radiation Measurements, 42*(1), 14–23. https://doi.org/10.1016/j.radmeas.2006.04.028
STCE Cosmic Rays. (2025). https://www.stce.be/content/sc25-tracking#cosmicrays
STCE Proton. (2025). https://www.stce.be/content/sc25-tracking#proton
Townsend, L. W. (2005). Implications of the space radiation environment for human exploration in deep space. *Radiation Protection Dosimetry, 115*(1–4), 44–50. https://doi.org/10.1093/rpd/nci141
Washburn, S. A., Blattnig, S. R., Singleterry, R. C., & Westover, S. C. (2015). Active magnetic radiation shielding system analysis and key technologies. *Life Sciences in Space Research, 5*, 22–43. https://doi.org/10.1016/j.lssr.2014.12.004
Xu, W., et al. (2021). A method for calculating atmospheric radiation produced by cosmic rays and solar particles. Space Weather, 19(12), e2021SW002735. https://doi.org/10.1029/2021SW002735
Zeitlin, C., Hassler, D. M., Cucinotta, F. A., Ehresmann, B., Wimmer-Schweingruber, R. F., Brinza, D. E., ... & Reitz, G. (2013). Measurements of energetic particle radiation in transit to Mars on the Mars Science Laboratory. *Science, 340*(6136), 1080–1084. https://doi.org/10.1126/science.1235989